

CrossMark
click for updatesCite this: *Chem. Sci.*, 2017, 8, 2337Received 4th November 2016
Accepted 17th December 2016

DOI: 10.1039/c6sc04893e

www.rsc.org/chemicalscience

Reactivity of a coordinated inorganic acetylene unit, HBNH, and the azidoborane cation $[\text{HB}(\text{N}_3)]^+\dagger$ Anindya K. Swarnakar, Christian Hering-Junghans, Michael J. Ferguson,
Robert McDonald and Eric Rivard*

A donor–acceptor complex of HBNH was prepared via thermolysis of a carbene-stabilized azidoborane. The reactivity of the fundamentally important HBNH unit (inorganic alkyne analogue) was explored in detail, including attempts to convert this species and related hydrido(azido)borane cations into molecular complexes of BN. This work provides added impetus for the development of molecular precursors that can release bulk boron nitride (a desirable insulator and thermal conductor) under mild conditions, and from solution.

Introduction

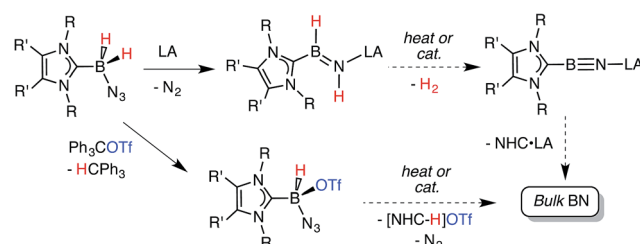
Iminoboranes ($\text{RB}\equiv\text{NR}'$) are inorganic isoelectronic counterparts to alkynes however their isolation is challenging due to the highly polar nature of their core B–N triple bonds, making these species vulnerable to cyclooligomerization.^{1,2} In seminal studies, Paetzold and coworkers used steric protection to obtain iminoboranes (*e.g.* $^t\text{BuB}\equiv\text{N}^t\text{Bu}$) as stable entities, and demonstrated initial coordination chemistry.^{2d} More recently, the Braunschweig, Bertrand and Stephan teams employed carbene-based donors to intercept reactive iminoboranes,³ including the halosilyl analogue ClBNSiMe_3 .^{3a} Despite these excellent studies, the parent iminoborane, HBNH, remained only identifiable in cryogenic matrices (40 K) or as a fleeting species in the gas phase,^{4,5} yet HBNH is of interest as a possible intermediate in the laser-induced dehydrogenative synthesis of boron nitride (BN) from $\text{H}_3\text{N}\cdot\text{BH}_3$.⁶

Recently our group was successful in intercepting the first example of a stable complex of HBNH by placing this unsaturated unit in between a sterically encumbered *N*-heterocyclic carbene (NHC) donor and a large triarylfluoroborane acceptor.^{7,8} Unfortunately the use of these bulky substituents restricted access to the HBNH array by potential reagents/catalysts. In this Edge Article we introduce a more reactive HBNH adduct and describe our attempts to convert this species into $\text{LB}\cdot\text{B}\equiv\text{N}\cdot\text{LA}$ complexes (LA = Lewis acid; LB = Lewis base; Scheme 1); in addition we investigate the reactivity of the donor-stabilized azidohydride boronium cation $[\text{BH}(\text{N}_3)]^+$.⁹ The ultimate goal of our program would be to use these newly

developed B–N species for the mild solution-based preparation of bulk boron nitride (Scheme 1). BN and its nanodimensional analogues are highly coveted in the context of advancing modern electronics due to their refractory nature, and desirable electronically insulating and heat dissipating properties.^{10,11}

Results and discussion

Our initial donor–acceptor HBNH complex $\text{IPr}\cdot\text{HB}=\text{NH}\cdot\text{BAR}^{\text{F}}_3$ [$\text{IPr} = [(\text{HCNDipp})_2\text{C}]$; $\text{Dipp} = 2,6\text{-}^i\text{Pr}_2\text{C}_6\text{H}_3$; $\text{Ar}^{\text{F}} = 3,5\text{-(F}_3\text{C)}_2\text{C}_6\text{H}_3$]^{7a} was generated by the Lewis acid (BAR^{F}_3) promoted loss of N_2 from the known boron azide $\text{IPr}\cdot\text{BH}_2\text{N}_3$,¹² followed by an intramolecular 1,2 hydride shift from B to N (Scheme 1). The presence of both hydridic ($\text{B}-\text{H}^{\delta-}$) and acidic ($\text{N}-\text{H}^{\delta+}$) residues in the HBNH unit prompted us to explore the dehydrogenation of this iminoborane species as a possible route to a molecular adduct of boron nitride, $\text{IPr}\cdot\text{B}\equiv\text{N}\cdot\text{BAR}^{\text{F}}_3$. However $\text{IPr}\cdot\text{HB}=\text{NH}\cdot\text{BAR}^{\text{F}}_3$ was found to be unreactive in the presence of common dehydrogenation pre-catalysts¹³ such as $[\text{Rh}(\text{COD})\text{Cl}]_2$ (COD = 1,5-cyclooctadiene).^{7a} The inertness of the iminoborane array was initially attributed to the presence of an extremely congested coordination environment. Thus we decided to generate an HBNH complex supported by the less hindered NHC, $\text{ImMe}_2^i\text{Pr}_2$ [$\text{ImMe}_2^i\text{Pr}_2 = (\text{MeCN}^i\text{Pr})_2\text{C}$].¹⁴



Scheme 1 Synthetic routes explored in this paper are each connected by a common goal of obtaining bulk BN under mild conditions.

Department of Chemistry, University of Alberta, 11227 Saskatchewan Drive, Edmonton, Alberta, Canada T6G 2G2. E-mail: erivard@ualberta.ca

† Electronic supplementary information (ESI) available: Experimental details and tables of crystallographic data for compounds 3–8 and 11. CCDC 1514190–1514196. For ESI and crystallographic data in CIF or other electronic format see DOI: 10.1039/c6sc04893e

The required azidoborane for our HBNH adduct synthesis, $\text{ImMe}_2^i\text{Pr}_2 \cdot \text{BH}_2\text{N}_3$ (**2**), was prepared from $\text{ImMe}_2^i\text{Pr}_2 \cdot \text{BH}_3$ ¹⁵ in two high yielding steps (Scheme 2). $\text{ImMe}_2^i\text{Pr}_2 \cdot \text{BH}_2\text{N}_3$ (**2**) was then combined with a stoichiometric amount of the fluoroarylborane, BAr^{F}_3 , followed by heating to 80 °C for 12 h in toluene to afford the target iminoborane adduct $\text{ImMe}_2^i\text{Pr}_2 \cdot \text{HB}=\text{NH} \cdot \text{BAr}^{\text{F}}_3$ (**3**) as a colorless solid in a 64% yield (mp = 142–146 °C). Based on prior studies^{7a} this reaction is believed to proceed *via* initial N_2 elimination and trapping of the resulting nitrene adduct, $\text{ImMe}_2^i\text{Pr}_2 \cdot \text{H}_2\text{B}=\text{N} \cdot \text{BAr}^{\text{F}}_3$ by a 1,2-hydride migration from B to N (Scheme 2). It is salient to mention that the generation of transient nitrenes from boron azides is known in the literature.^{1a,16}

As expected, the $^1\text{H}\{^{11}\text{B}\}$ NMR spectrum of $\text{ImMe}_2^i\text{Pr}_2 \cdot \text{HB}=\text{NH} \cdot \text{BAr}^{\text{F}}_3$ (**3**) gave discernable N–H and B–H resonances at 5.42 and 4.62 ppm, respectively (in C_6D_6), which are similar to the corresponding resonances found in $\text{IPr} \cdot \text{HB}=\text{NH} \cdot \text{BAr}^{\text{F}}_3$.^{7a} X-ray crystallography later conclusively identified the presence of an $\text{HB}=\text{NH}$ moiety in **3** (Fig. 1). The core iminoborane unit in **3** adopts a *trans* arrangement [C–B–N–B dihedral angle = 178.1(2)°] thereby minimizing intramolecular repulsion between the $\text{ImMe}_2^i\text{Pr}_2$ and BAr^{F}_3 groups. The central B=N and C_(NHC)–B bond distances in **3** are 1.369(3) Å and 1.596(4) Å, which are the same within experimental error as in $\text{IPr} \cdot \text{HB}=\text{NH} \cdot \text{BAr}^{\text{F}}_3$.^{7a} A slightly elongated B–N distance was reported in the iminoborane $(\text{HC}\equiv\text{C})_2\text{B}=\text{N}^i\text{Pr}_2$ (1.385(3) Å).¹⁷

$\text{ImMe}_2^i\text{Pr}_2 \cdot \text{HB}=\text{NH} \cdot \text{BAr}^{\text{F}}_3$ (**3**) was examined by computational methods and an overall charge of $-0.13e$ was found for the central $\text{HB}=\text{NH}$ moiety. As anticipated, the B=N linkage (Wiberg bond index, WBI = 1.33) has considerable polarization of the σ - and π -components towards N (*ca.* 80% located on N), according to NBO analysis. The LUMO shows B–N π^* and B–C π -character, while contributions to the B–N π -manifold appear in HOMO–2 and HOMO–6 (Fig. 2).¹⁸ The computed HOMO–LUMO gap is 173 kcal mol^{–1} and is in agreement with the observed inertness of **3** (*vide infra*).

With the less hindered HBNH complex **3** in hand, we attempted to promote its dehydrogenation to afford the BN adduct $\text{ImMe}_2^i\text{Pr}_2 \cdot \text{B}\equiv\text{N} \cdot \text{BAr}^{\text{F}}_3$. When compound **3** was treated with the well-known dehydrogenation pre-catalyst $[\text{Rh}(\text{COD})\text{Cl}]_2$

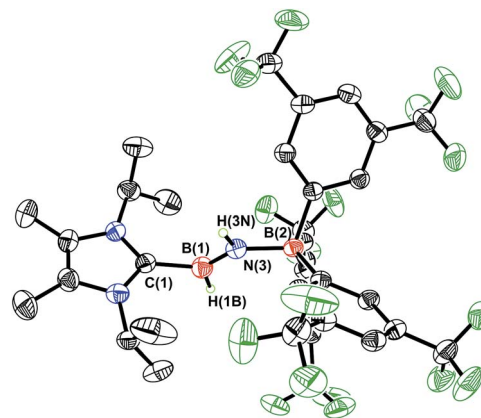
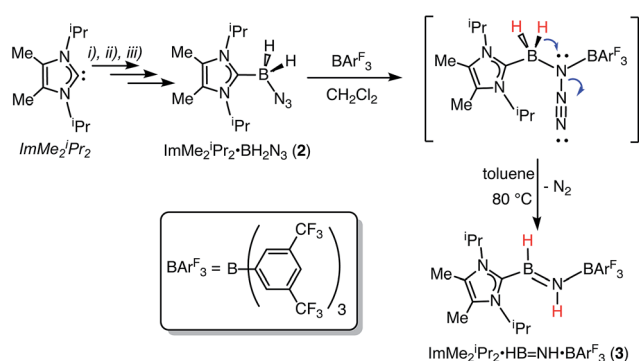


Fig. 1 Molecular structure of $\text{ImMe}_2^i\text{Pr}_2 \cdot \text{HB}=\text{NH} \cdot \text{BAr}^{\text{F}}_3$ (**3**) with thermal ellipsoids presented at a 30% probability level. All carbon-bound hydrogen atoms have been omitted for clarity. Selected bond lengths (Å) and angles (deg): C(1)–B(1) 1.596(2), B(1)–N(3) 1.369(3), N(3)–B(2) 1.572(2); C(1)–B(1)–N(3) 121.8(2), B(1)–N(3)–B(2) 130.5(2), N(3)–B(1)–H(1B) 125.2(16), B(1)–N(3)–H(3N) 115.8(19).

(2–5 mol%) in toluene, no reaction occurred at room temperature. When the same dehydrogenation reaction was attempted at 90 °C for 7 days, only partial decomposition of **3** (<10%; $[\text{ImMe}_2^i\text{Pr}_2\text{–H}]^+$ salt) was noted. Moreover, compound **3** was also combined with the potential dehydrogenation catalyst $\text{CpFe}(\text{CO})_2\text{OTf}$ and the Frustrated Lewis Pair (FLP), $^t\text{Bu}_3\text{P}$ and BAr^{F}_3 , (both known to promote H_2 loss from amine-boranes) however in each case no reaction with **3** transpired. Likewise attempted H_2 release from **3** by photolysis (300 W Hg lamp in Et_2O) gave no reaction.

Undaunted by the lack of thermally- or catalytically-instigated H_2 release from **3**, we decided to see if the core HBNH unit underwent chemical transformations one would expect for a polarized B=N linkage.¹⁹ When $\text{ImMe}_2^i\text{Pr}_2 \cdot \text{HB}=\text{NH} \cdot \text{BAr}^{\text{F}}_3$ (**3**) was combined with one equivalent of HCl in Et_2O , the resulting ^{11}B NMR spectrum was consistent with the presence



Scheme 2 Synthesis of $\text{ImMe}_2^i\text{Pr}_2 \cdot \text{HB}=\text{NH} \cdot \text{BAr}^{\text{F}}_3$ (**3**) starting from the azidoborane adduct $\text{ImMe}_2^i\text{Pr}_2 \cdot \text{BH}_2\text{N}_3$ (**2**). Reagents: (i) $\text{THF} \cdot \text{BH}_3$, THF, rt (95% yield); (ii) 0.5 equiv. I_2 , benzene, rt (90% yield); (iii) NaN_3 , DMSO, rt (68% yield).

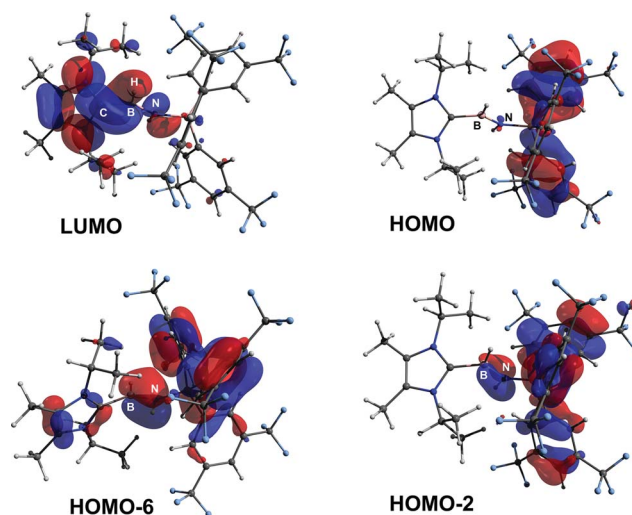


Fig. 2 POV-ray depiction of selected Kohn–Sham orbitals of **3**.



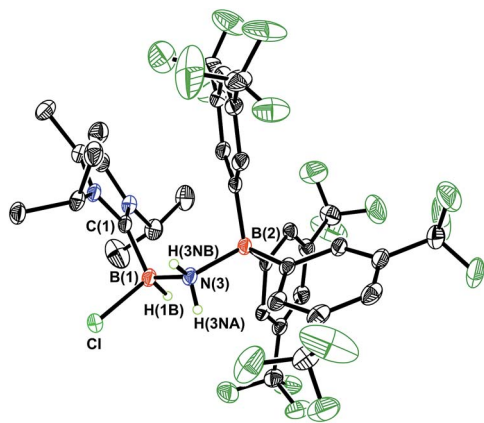


Fig. 3 Molecular structure of $\text{ImMe}_2^i\text{Pr}_2 \cdot \text{H}(\text{Cl})\text{B-NH}_2 \cdot \text{BARF}_3$ (**4**) with thermal ellipsoids presented at a 30% probability level. All carbon-bound hydrogen atoms have been omitted for clarity. Selected bond lengths (Å) and angles (deg): C(1)–B(1) 1.616(5), B(1)–N(3) 1.585(4), N(3)–B(2) 1.632(4), B(1)–Cl 1.906(4); C(1)–B(1)–N(3) 115.7(3), B(1)–N(3)–B(2) 124.4(2), N(3)–B(1)–Cl 107.2(2), B(1)–N(3)–H(3NA) 105(2).

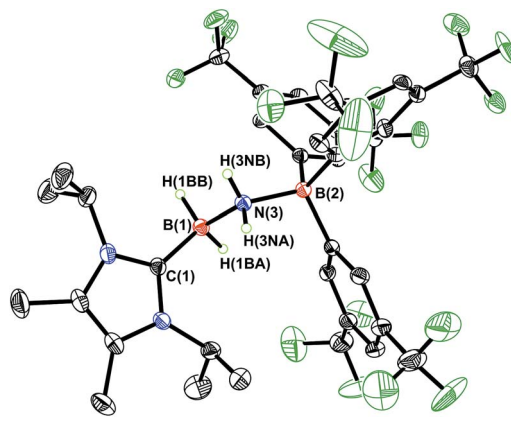
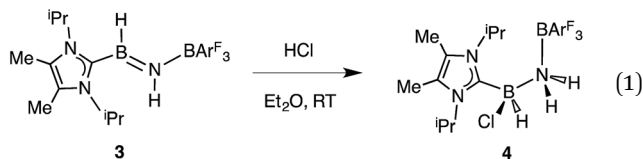


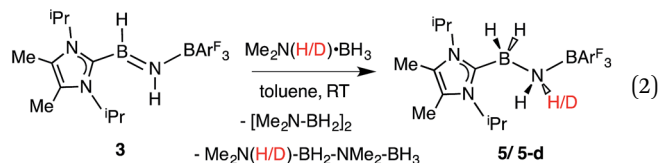
Fig. 4 Molecular structure of $\text{ImMe}_2^i\text{Pr}_2 \cdot \text{H}_2\text{B-NH}_2 \cdot \text{BARF}_3$ (**5**) with thermal ellipsoids presented at a 30% probability level. All carbon-bound hydrogen atoms have been omitted for clarity. Selected bond lengths (Å) and angles (deg): C(1)–B(1) 1.627(3), B(1)–N(3) 1.613(3), N(3)–B(2) 1.622(2); C(1)–B(1)–N(3) 110.23(15), B(1)–N(3)–B(2) 120.11(14), N(3)–B(1)–H(1BB) 109.0(12), B(1)–N(3)–H(3NA) 106.8(15).

of two four-coordinate boron centers ($\delta = -3.7$ and -9.5 ppm in C_6D_6). X-ray crystallography confirmed the successful addition of HCl across the $\text{B}=\text{N}$ bond to form $\text{ImMe}_2^i\text{Pr}_2 \cdot \text{H}(\text{Cl})\text{B-NH}_2 \cdot \text{BARF}_3$ (**4**) as a racemic mixture due to the presence of a chiral boron atom (Fig. 3; eqn (1)). The addition of chloride at the boron center in **4** illustrates the Lewis acidic nature of the boron atom in coordinated $\text{HB}=\text{NH}$ in **3**. The central B–N bond distance in **4** is 1.585(4) Å and is comparable to the B–N bond lengths found in structurally related amine-boranes, such as $\text{IPr} \cdot \text{BH}_2\text{NH}_2\text{BH}_3$.²⁰ The $\text{C}_{(\text{NHC})}$ –B bond distance in **4** is 1.616(5) Å which, somewhat to our surprise, is similar in length as the corresponding $\text{C}_{(\text{NHC})}$ –B bond distance of 1.596(4) Å in **3**, despite the change in hybridization at boron to sp^3 in **4**; however, the capping N-BARF_3 interaction in **4** (1.632(4) Å) is longer than in the HBNH adduct **3** (1.572(2) Å). Addition of HCl also leads to a substantial canting of the relative arrangement of the capping NHC and borane groups (vs. in **3**), as evidenced by the C–B–N–B dihedral angle of 65.3(3)°.



While the polarized $\text{B}=\text{N}$ linkage in $\text{ImMe}_2^i\text{Pr}_2 \cdot \text{HB}=\text{NH} \cdot \text{BARF}_3$ (**3**) did not exhibit Frustrated Lewis Pair (FLP) type reactivity with H_2 , CO or CO_2 ,²¹ effective transfer hydrogenation²² occurred between the amine-borane $\text{Me}_2\text{NH} \cdot \text{BH}_3$ and **3** (eqn (2)). The resulting hydrogenated product $\text{ImMe}_2^i\text{Pr}_2 \cdot \text{H}_2\text{B-NH}_2 \cdot \text{BARF}_3$ (**5**) formed after 12 h at room temperature; the expected dehydrogenated by-products $[\text{Me}_2\text{N-BH}_2]_2$ and $\text{Me}_2\text{NH-BH}_2\text{-NMe}_2\text{-BH}_3$ were also detected by NMR spectroscopy. To probe the mechanism of this transformation in

more detail, compound **3** was combined with $\text{Me}_2\text{ND} \cdot \text{BH}_3$; the resulting product $\text{ImMe}_2^i\text{Pr}_2 \cdot \text{H}_2\text{B-N}(\text{H})\text{D} \cdot \text{BARF}_3$ (**5-d**)¹⁸ suggested direct H/D atom transfer from B to B and N to N.^{22a} The molecular structure of **5** (Fig. 4) has similar overall structural features as the HCl addition product $\text{ImMe}_2^i\text{Pr}_2 \cdot \text{H}(\text{Cl})\text{B-NH}_2 \cdot \text{BARF}_3$ (**4**) with an elongated $\text{C}_{\text{NHC}}\text{-B}$ distance of 1.627(3) Å in accordance with the decreased electrophilicity of the $\text{BH}_2\text{-NH}_2\text{-BARF}_3$ unit in **5**.



Despite the presence of both hydridic and acidic H atoms in $\text{ImMe}_2^i\text{Pr}_2 \cdot \text{H}_2\text{B-NH}_2 \cdot \text{BARF}_3$ (**5**), our efforts to induce dehydrogenation (and reform the HBNH adduct **3**) by heating up to 100 °C in the presence of known dehydrogenation pre-catalysts $[\text{Rh}(\text{COD})\text{Cl}]_2$ or $\text{CpFe}(\text{CO})_2\text{OTf}$ led to no discernable reaction. Furthermore, **5** remained unreactive towards the possible H_2 acceptors, $\text{PhN}=\text{NPh}$ and the FLP ($^t\text{Bu}_3\text{P}/\text{BARF}_3$), and did not yield **3** upon attempted photolysis (300 W Hg lamp). Accordingly, the calculated NPA charges for **5** show less hydridic character for the B–H array (-0.009 and $-0.020e$) compared to the reactive amine-borane $\text{MeNH}_2 \cdot \text{BH}_3$ (B–H charges of -0.030 to $-0.034e$), thus partially explaining the higher reactivity for the latter species. The computed positive charges for N-bound hydrogen atoms in **5** (0.429 and 0.437 e) are similar to those in $\text{MeNH}_2 \cdot \text{BH}_3$.¹⁸

In order to directly probe the Lewis acidity of the HBNH unit in **3**,²³ an additional equivalent of the carbene donor $\text{ImMe}_2^i\text{Pr}_2$ was combined with $\text{ImMe}_2^i\text{Pr}_2 \cdot \text{HB}=\text{NH} \cdot \text{BARF}_3$ (**3**). While the expected bis adduct $(\text{ImMe}_2^i\text{Pr}_2)_2\text{HBNH} \cdot \text{BARF}_3$ (**6**) could be isolated in the solid state as a yellow solid (88% yield)



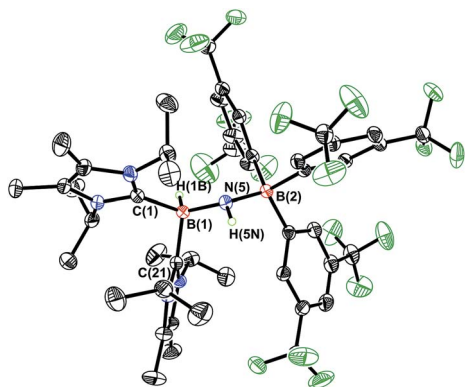
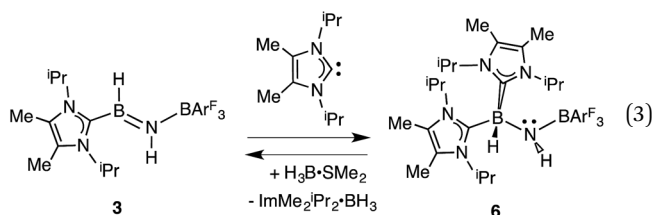


Fig. 5 Molecular structure of $[\text{ImMe}_2^{\text{iPr}_2}]_2 \cdot \text{HB-NH} \cdot \text{BARF}_3$ (**6**) with thermal ellipsoids presented at a 30% probability level. All carbon-bound hydrogen atoms have been omitted for clarity. Selected bond lengths (Å) and angles (deg): C(1)–B(1) 1.684(3), C(21)–B(1) 1.660(2), B(1)–N(5) 1.512(2), N(5)–B(2) 1.539(2); C(1)–B(1)–N(5) 117.28(14), B(1)–N(5)–B(2) 125.03(14), N(5)–B(1)–C(21) 112.26(14), N(5)–B(1)–H(1B) 113.4(11), B(1)–N(5)–H(5N) 112.5(14).

and characterized by X-ray crystallography (Fig. 5, *vide infra*), the NMR spectra of this product in solution exhibited dynamic behavior, consistent with partial dissociation of one NHC ligand. Addition of the Lewis acid acceptor BH_3 (delivered in the form of $\text{Me}_2\text{S} \cdot \text{BH}_3$) led to the quantitative removal of one equiv. of $\text{ImMe}_2^{\text{iPr}_2}$ from **6** to reform **3** (eqn (3)). Consistent with weaker overall $\text{C}_{\text{NHC}}\text{--B}$ interactions in **6** relative to in the HBNH adduct **3**, elongated distances of 1.684(3) and 1.660(2) Å were found in **6** (by *ca.* 0.06–0.08 Å). For comparison, the C–B distances in Bertrand's mixed NHC/CAAC complex $[\text{CAAC} \cdot \text{B}(\text{L})\text{H}(\text{OTf})]\text{BPh}_4$ [CAAC = cyclic alkyl(amino) carbene; L = benzoimidazolylidene] were slightly shorter (1.645(2) and 1.627(2) Å).²⁴ Coordination of two NHCs at boron in **6** resulted in substantial lengthening of the core B–N distance from a value of 1.369(3) in **3** to 1.512(2) Å, suggesting a lack of a B–N π -bond interaction in **6**. Our computational studies on **6** support this postulate with a computed B–N Wiberg bond index (WBI) of 0.85 (*vs.* 1.33 in **3**). Moreover, interaction of the Lewis base $\text{ImMe}_2^{\text{iPr}_2}$ with the LUMO in **3** populates an orbital with B–N π^* -character (Fig. 2).¹⁸

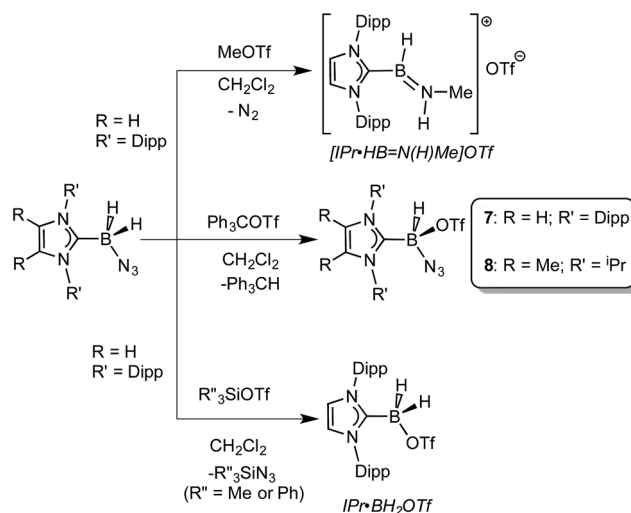


Prior work in our group showed that N_2 loss/1,2-hydride migration in $\text{IPr} \cdot \text{BH}_2\text{N}_3$ could also be instigated with the methylating agent MeOTf (Scheme 3), eventually leading to the formation of $[\text{IPr} \cdot \text{HB}=\text{N}(\text{Me})\text{H}]\text{OTf}$.^{7a} Accordingly we wanted to expand the range of known electrophiles that could trigger this potentially general transformation. However, with Ph_3COTf and R_3SiOTf ($\text{R} = \text{Me}$ and Ph), divergent reactivity was uncovered

(Scheme 3). Specifically, when $\text{IPr} \cdot \text{BH}_2\text{N}_3$ or the less hindered analogue $\text{ImMe}_2^{\text{iPr}_2} \cdot \text{BH}_2\text{N}_3$ (**2**) was combined with Ph_3COTf in CH_2Cl_2 , hydride abstraction occurred to yield triphenylmethane (Ph_3CH) and the new azido(hydrido)borane adducts $\text{IPr} \cdot \text{B} \cdot \text{H}(\text{OTf})\text{N}_3$ (**7**) and $\text{ImMe}_2^{\text{iPr}_2} \cdot \text{B} \cdot \text{H}(\text{OTf})\text{N}_3$ (**8**) in isolated yields of 95 and 66%, respectively (see Fig. 6 and S1† for the corresponding X-ray structures).¹⁸ The ^{19}F NMR spectra of **7** and **8** show the retention of strong B–OTf contacts in solution (*e.g.* $\delta = -76.9$ ppm for **7** in C_6D_6), while intense azide IR stretches were present at 2117 and 2116 cm^{-1} for compounds **7** and **8**, respectively; these values compare well with the $\nu(\text{N}_3)$ of 2117 cm^{-1} reported for Cummins' azido borate salt $[\text{tBu}_4\text{N}][(\text{N}_3)\text{B}(\text{C}_6\text{F}_5)_3]$.²⁵ Thus by simply replacing MeOTf with Ph_3COTf , H/OTf exchange chemistry can transpire in place of N_2 loss.

Yet another reaction pathway occurred when $\text{IPr} \cdot \text{BH}_2\text{N}_3$ was combined with the silyltriflates Me_3SiOTf and Ph_3SiOTf (Scheme 3). In each case, complete OTf/azide exchange transpired to form the corresponding silylazides (Me_3SiN_3 and Ph_3SiN_3 ; identified by NMR spectroscopy) and the known borane adduct $\text{IPr} \cdot \text{BH}_2\text{OTf}$.¹² It appears that N_3/OTf exchange is driven by the relatively strong Si–N bonds (*ca.* 355 kJ mol^{-1})²⁶ in relation to the C–N linkages (*ca.* 305 kJ mol^{-1}), thus azide abstraction by Ph_3C^+ sources is not as favorable. To recap, $\text{NHC} \cdot \text{BH}_2\text{N}_3$ shows three distinct possible reactivity pathways in the presence of electrophiles: (a) HBNH formation *via* N_2 loss/1,2-H shift; (b) hydride abstraction; (c) azide abstraction.

The accidentally uncovered high yield syntheses of the $\text{NHC} \cdot \text{BH}(\text{OTf})\text{N}_3$ adducts **7** and **8** (Scheme 3) opened another possible path to boron nitride (BN). Motivated by the balanced equation $\text{NHC} \cdot \text{BH}(\text{OTf})\text{N}_3 \rightarrow \text{BN} + \text{N}_2 + [\text{NHC-H}]\text{OTf}$; Scheme 1) we decided to investigate the reactivity of both **7** and **8** in more detail. Initially we explored the direct thermolysis of **7** and **8** in solution at temperatures approaching 100 °C (**Caution!**) but these adducts proved to be stable under these conditions. Treatment of **8** with potassium as a reducing agent (in order to



Scheme 3 Divergent reactivity of $\text{NHC} \cdot \text{BH}_2\text{N}_3$ adducts with MeOTf, $\text{R}'_3\text{SiOTf}$ ($\text{R}'' = \text{Me}$ or Ph), and Ph_3COTf .

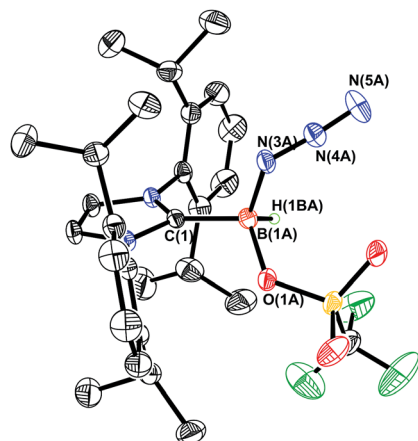


Fig. 6 Molecular structure of IPr·BHN₃(OTf) (7) with thermal ellipsoids presented at a 30% probability level. All carbon-bound hydrogen atoms have been omitted for clarity. Selected bond lengths (Å) and angles (deg) with parameters associated with a second molecule in the asymmetric unit listed in square brackets: C(1)–B(1A) 1.590(11) [1.652(10)], B(1A)–N(3A) 1.542(8) [1.482(12)], N(3A)–N(4A) 1.223(7) [1.211(8)], N(4A)–N(5A) 1.168(9) [1.145(11)], B(1A)–O(1A) 1.552(11) [1.562(11)]; N(3A)–N(4A)–N(5A) 175.0(11) [178.2(11)].

promote the possible reaction: $8 + K \rightarrow \frac{1}{2}H_2 + N_2 + KOTf + BN + NHC$) produced the free carbene ImMe₂ⁱPr₂ as the only soluble product by NMR spectroscopy. Whereas the reaction of **8** with KC₈ produced three different carbene containing products: free carbene ImMe₂ⁱPr₂, ImMe₂ⁱPr₂·BH₂N₃ and ImMe₂ⁱPr₂·BH₃.²⁷ Analysis of the insoluble fractions from both of the reactions by IR identified the presence of K[N₃] and K[OTf], indicating that B–N(azide) bond scission transpired in place of H₂ loss and boron nitride formation; in support of this reaction path, no IR bands for bulk BN could be found in the product mixture. Furthermore, the LUMO computed for the model species ImMe₂·B(H)N₃(OTf) (ImMe₂ = (HCNMe)₂C:) revealed B–N σ*-character, thus explaining the preferential B–N bond scission noted upon reduction.¹⁸

In order to induce 1,2-H transfer in the NHC·BHN₃(OTf) species **7** and **8** the donor ImMe₂ⁱPr₂ (ref. 28) was added to form the respective bis(carbene) boronium salts [IPr(ImMe₂ⁱPr₂)·BH(N₃)]OTf (**9**) and [(ImMe₂ⁱPr₂)₂·BH(N₃)]OTf (**10**) (eqn (4)). The spectral parameters of these salts were consistent with free OTf[−] counteranions (e.g. ¹⁹F resonance at −78.1 ppm for **10** in CDCl₃) and the retention of boron-bound azide and hydride substituents (e.g. IR stretches at ca. 2107 and 2400 cm^{−1} for **9**). Structural confirmation of the proposed bonding environment was provided by an X-ray structure of the tetraarylfuoroborate salt [(ImMe₂ⁱPr₂)₂·BH(N₃)]BAR₄^F (**11**) (eqn (5); Fig. 7). With the goal of taking advantage of possibly higher nucleophilic character of the azide group in **11** in relation to the mono-carbene congener **8**, we combined **11** with one equivalent of BAR₃^F. In place of observing Lewis acid-assisted N₂ elimination/H-migration to give the “trapped” BNH adduct [(ImMe₂ⁱPr₂)₂·B=NH·BAR₃^F]OTf, no reaction transpired. Likewise no conversion of **11** was noted upon heating this species with BAR₃^F at 90–100 °C or under UV irradiation.

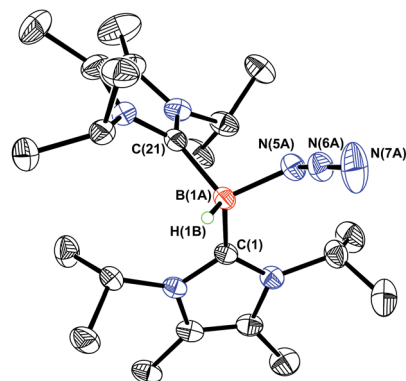
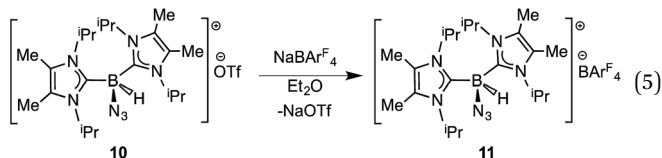
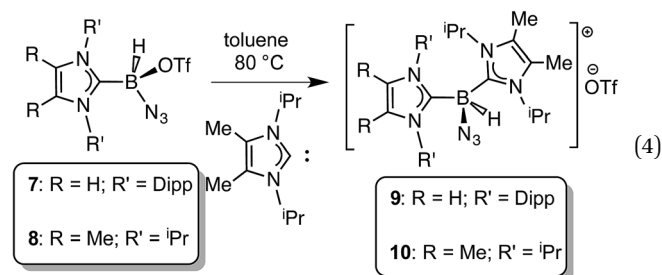


Fig. 7 Molecular structure of [(ImMe₂ⁱPr₂)₂·BHN₃][B(C₆H₃(*m*-CF₃)₂)₄] (**11**) with thermal ellipsoids presented at a 30% probability level. All carbon-bound hydrogen atoms and BAR₄^F anion have been omitted for clarity. Selected bond lengths (Å) and angles (deg) with parameters associated with a second molecule in the asymmetric unit listed in square brackets: C(1)–B(1A) 1.642(9) [1.71(3)], C(21)–B(1A) 1.650(9) [1.59(3)], B(1A)–N(5A) 1.553(7) [1.514(13)], N(5A)–N(6A) 1.202(6) [1.206(11)], N(6A)–N(7A) 1.147(10) [1.159(14)]; N(5A)–N(6A)–N(7A) 173.7(6) [158(2)].



Conclusion

In this article we present efficient methods to prepare complexes of HBNH and [HB(N₃)]⁺, starting from readily available carbene-azidoborane adducts. In addition, this study provides key insights into the reactivity of the fundamentally important HBNH unit, an inorganic analogue of acetylene. While our detailed investigations aimed at forming bulk boron nitride (BN) from these species under mild conditions were not directly successful, we hope that this work inspires others to seek low temperature (<200 °C) routes to this inorganic wide band gap material. By suitable modification of the capping stabilizing groups, related B–N sources could be potentially used as building blocks for the rational construction of boron nitride materials and π-extended structures.²⁹



Acknowledgements

This work was supported by the Natural Sciences and Engineering Research Council of Canada (Discovery Grant and CREATE grants for E. R.; CREATE fellowship for A. K. S.), and the Canada Foundation for Innovation (CFI). C. H.-J. acknowledges the Alexander von Humboldt Foundation for a Feodor-Lynen Postdoctoral Fellowship. The authors also acknowledge Mark Miskolzie and Nupur Dabral for experimental assistance. The authors also thank Matthew M. D. Roy and Dr Urmibhusan Bhakta for helpful discussions.

References

- (a) P. Paetzold, *Adv. Inorg. Chem.*, 1987, **31**, 123; (b) H. Nöth, *Angew. Chem., Int. Ed. Engl.*, 1988, **27**, 1603; (c) R. C. Fischer and P. P. Power, *Chem. Rev.*, 2010, **110**, 3877; (d) H. Braunschweig, R. D. Dewhurst and A. Schneider, *Chem. Rev.*, 2010, **110**, 3924; (e) O. Ayhan, T. Eckert, F. A. Plamper and H. Helten, *Angew. Chem., Int. Ed.*, 2016, **55**, 13321.
- (a) P. Paetzold and C. von Plotho, *Chem. Ber.*, 1982, **115**, 2819; (b) H.-U. Meier, P. Paetzold and E. Schröder, *Chem. Ber.*, 1984, **117**, 1954; (c) J. Kiesgen, J. Münster and P. Paetzold, *Chem. Ber.*, 1993, **126**, 1559; (d) E. Bulak, G. E. Herberich, I. Manners, H. Mayer and P. Paetzold, *Angew. Chem., Int. Ed. Engl.*, 1988, **27**, 958.
- (a) F. Dahcheh, D. Martin, D. W. Stephan and G. Bertrand, *Angew. Chem., Int. Ed.*, 2014, **53**, 13159; (b) F. Dahcheh, D. W. Stephan and G. Bertrand, *Chem.-Eur. J.*, 2015, **21**, 199; (c) H. Braunschweig, W. C. Ewing, K. Geetharani and M. Schäfer, *Angew. Chem., Int. Ed.*, 2015, **54**, 1662.
- (a) E. R. Lory and R. F. Porter, *J. Am. Chem. Soc.*, 1973, **95**, 1766; (b) Y. Kawashima, K. Kawaguchi and E. Hirota, *J. Chem. Phys.*, 1987, **87**, 6331; (c) C. A. Thompson and L. Andrews, *J. Am. Chem. Soc.*, 1995, **117**, 10125; (d) F. Zhang, P. Maksyutenko, R. I. Kaiser, A. M. Mebel, A. Gregusova, S. A. Perera and R. J. Bartlett, *J. Phys. Chem. A*, 2010, **114**, 12148.
- For selected computational studies on HBNH, see: (a) N. C. Baird and R. K. Datta, *Inorg. Chem.*, 1972, **11**, 17; (b) M. H. Matus, D. J. Grant, M. T. Nguyen and D. A. Dixon, *J. Phys. Chem. C*, 2009, **113**, 16553; (c) R. Sundaram, S. Scheiner, A. K. Roy and T. Kar, *J. Phys. Chem. C*, 2015, **119**, 3253.
- H. Liu, P. Jin, Y.-M. Xue, C. Dong, X. Li, C.-C. Tang and X.-W. Du, *Angew. Chem., Int. Ed.*, 2015, **54**, 7051.
- (a) A. K. Swarnakar, C. Hering-Junghans, K. Nagata, M. J. Ferguson, R. McDonald, N. Tokitoh and E. Rivard, *Angew. Chem., Int. Ed.*, 2015, **54**, 10666; (b) Our HBNH adducts can also be considered as analogues of known Frustrated Lewis Pair (FLP) complexes of alkynes, see: M. A. Dureen and D. W. Stephan, *J. Am. Chem. Soc.*, 2009, **131**, 8396.
- For related examples of donor-acceptor stabilization of main group species, see: (a) U. Vogel, A. Y. Timoshkin and M. Scheer, *Angew. Chem., Int. Ed.*, 2001, **40**, 4409; (b) P. A. Rugar, M. C. Jennings, P. J. Ragogna and K. M. Baines, *Organometallics*, 2007, **26**, 4109; (c) S. M. I. Al-Rafia, A. C. Malcolm, R. McDonald, M. J. Ferguson and E. Rivard, *Angew. Chem., Int. Ed.*, 2011, **50**, 8354; (d) T. Yamaguchi, A. Sekiguchi and M. Driess, *J. Am. Chem. Soc.*, 2010, **132**, 14061; (e) A. C. Filippou, B. Baars, O. Chernov, Y. N. Lebedev and G. Schnakenburg, *Angew. Chem., Int. Ed.*, 2014, **53**, 565; (f) Y.-P. Zhou, M. Karni, S. Yao, Y. Apeloig and M. Driess, *Angew. Chem., Int. Ed.*, 2016, **55**, 15096.
- For a computational study on LB·BN·LA species, see: M. R. Momeni, L. Shulman, E. Rivard and A. Brown, *Phys. Chem. Chem. Phys.*, 2015, **17**, 16525.
- (a) Y. Tian, B. Xu, D. Yu, Y. Ma, Y. Wang, Y. Jiang, W. Hu, C. Tang, Y. Gao, K. Luo, Z. Zhao, L.-M. Wang, B. Wen, J. He and Z. Liu, *Nature*, 2013, **493**, 385; (b) V. L. Solozhenko, O. O. Kurakevych and Y. Le Godec, *Adv. Mater.*, 2012, **24**, 1540; (c) H. Sumiya, S. Uesaka and S. Satoh, *J. Mater. Sci.*, 2000, **35**, 1181; (d) Y. Kubota, K. Watanabe, O. Tsuda and T. Taniguchi, *Science*, 2007, **317**, 932; (e) K. Watanabe, T. Taniguchi, T. Niiyama, K. Miya and M. Taniguchi, *Nat. Photonics*, 2009, **3**, 591; (f) S. Bernard, C. Salameh and P. Miele, *Dalton Trans.*, 2016, **45**, 861.
- Our group has used LB·GeH₂·LA complexes as precursors to both bulk germanium and luminescent nanoparticles: (a) E. Rivard, *Dalton Trans.*, 2014, **43**, 8577; (b) T. K. Purkait, A. K. Swarnakar, G. B. De Los Reyes, F. A. Hegmann, E. Rivard and J. G. C. Veinot, *Nanoscale*, 2015, **7**, 2241.
- A. Solov'yev, Q. Chu, S. J. Geib, L. Fensterbank, M. Malacria, E. Lacôte and D. P. Curran, *J. Am. Chem. Soc.*, 2010, **132**, 15072.
- (a) C. A. Jaska, K. Temple, A. J. Lough and I. Manners, *J. Am. Chem. Soc.*, 2003, **125**, 9424; (b) E. M. Leitao, T. Jurca and I. Manners, *Nat. Chem.*, 2013, **5**, 817.
- N. Kuhn and T. Kratz, *Synthesis*, 1993, 561.
- N. Kuhn, G. Henkel, T. Kratz, J. Kreutzberg, R. Boese and A. H. Maulitz, *Chem. Ber.*, 1993, **126**, 2041.
- (a) M. Müller, C. Maichle-Mössmer and H. F. Bettinger, *Chem. Commun.*, 2013, **49**, 11773; (b) M. Müller, C. Maichle-Mössmer and H. F. Bettinger, *Angew. Chem., Int. Ed.*, 2014, **53**, 9380.
- F. Ge, G. Kehr, C. G. Daniliuc, C. Mück-Lichtenfeld and G. Erker, *Organometallics*, 2015, **34**, 4205.
- For complete synthetic, crystallographic and computational details, see the ESI.†
- (a) A. W. Laubengayer, O. T. Beachley Jr and R. F. Porter, *Inorg. Chem.*, 1965, **4**, 578; (b) O. T. Beachley Jr and B. Washburn, *Inorg. Chem.*, 1975, **14**, 120.
- A. C. Malcolm, K. J. Sabourin, R. McDonald, M. J. Ferguson and E. Rivard, *Inorg. Chem.*, 2012, **51**, 12905.
- (a) V. Sumerin, F. Schulz, M. Atsumi, C. Wang, M. Nieger, M. Leskelä, T. Repo, P. Pykkö and B. Rieger, *J. Am. Chem. Soc.*, 2008, **130**, 14117; (b) M.-A. Legaré, M.-A. Courtemanche, E. Rochette and F.-G. Fontaine, *Science*, 2015, **349**, 513; (c) T. Wang, G. Kehr, L. Liu, S. Grimme, C. G. Daniliuc and G. Erker, *J. Am. Chem. Soc.*, 2016, **138**, 4302; (d) Z. Mo, A. Rit, J. Campos, E. L. Kolychev



- and S. Aldridge, *J. Am. Chem. Soc.*, 2016, **138**, 3306; (e) D. W. Stephan, *Acc. Chem. Res.*, 2015, **48**, 306.
- 22 For related examples of transfer hydrogenation between amine-boranes and unsaturated B–N compounds, see: (a) A. P. M. Robertson, E. M. Leitao and I. Manners, *J. Am. Chem. Soc.*, 2011, **133**, 19322; (b) M. W. Lui, N. R. Paisley, R. McDonald, M. J. Ferguson and E. Rivard, *Chem.–Eur. J.*, 2016, **22**, 2134; (c) E. M. Leitao, N. E. Stubbs, A. P. M. Robertson, H. Helten, R. J. Cox, G. C. Lloyd-Jones and I. Manners, *J. Am. Chem. Soc.*, 2012, **134**, 16805.
- 23 We also explored the possible Lewis basic nature of **3**. When **3** was combined with CuI and BArF₃, no reaction was found; treatment of **3** with Me₂S·BH₃ (as a source of BH₃) gave a complicated product mixture.
- 24 D. A. Ruiz, M. Melaimi and G. Bertrand, *Chem. Commun.*, 2014, **50**, 7837.
- 25 A. R. Fox and C. C. Cummins, *J. Am. Chem. Soc.*, 2009, **131**, 5716.
- 26 (a) S. W. Benson, *J. Chem. Educ.*, 1965, **42**, 502; (b) R. Walsh, *Acc. Chem. Res.*, 1981, **14**, 246.
- 27 For the synthesis of BN by treating [XBNH]₃ (X = Cl or Br) with molten alkali metals, see: (a) E. J. M. Hamilton, S. E. Dolan, C. M. Mann, H. O. Colijn, C. A. McDonald and S. G. Shore, *Science*, 1993, **260**, 659; (b) E. J. M. Hamilton, S. E. Dolan, C. M. Mann, H. O. Colijn and S. G. Shore, *Chem. Mater.*, 1995, **7**, 111.
- 28 We have computed the charge of the boron-bound hydrogen atom in the model species [(ImMe₂)₂BH(N₃)]⁺ (see the ESI†) and noted slightly acidic character (NPA = +0.010); attempts to promote BN formation from **9** by treatment with sodium metal in Et₂O yielded free ImMe₂ⁱPr₂ with no sign of bulk BN formation by IR spectroscopy.
- 29 (a) M. J. S. Dewar, V. P. Kubba and R. Pettit, *J. Chem. Soc.*, 1958, 3073; (b) D. J. H. Emslie, W. E. Piers and M. Parvez, *Angew. Chem., Int. Ed.*, 2003, **42**, 1252; (c) P. G. Campbell, A. J. V. Marwitz and S.-Y. Liu, *Angew. Chem., Int. Ed.*, 2012, **51**, 6074; (d) K. Edel, S. A. Brough, A. N. Lamm, S.-Y. Liu and H. F. Bettinger, *Angew. Chem., Int. Ed.*, 2015, **54**, 7819.

